# Modeling of Vibrating Atomic Force Microscope's Cantilever within Different Frames of Reference

E. Kamau[1] and F. Voigt*,[1]
[1]University of Oldenburg

*Corresponding author:
Department of Computing Science , Division Microrobotics and Control Engineering
Uhlhornsweg 84, D-26111 Oldenburg, Germany, felix.voigt@uni-oldenburg.de

**Abstract:** Cantilever vibration modes were simulated with the finite element analysis and solver software package COMSOL. In the 1st approach the model consisted in an excitation piezo, a holder plate and a chip where the cantilever was mounted on. A sinusoidal voltage signal was applied to the piezo in the simulation, which resulted in movements of the holder plate and finally led to the excitation of the cantilever. In the 2nd approach the model consisted only in a holder plate and the chip with the cantilever. The cantilever chip was examined in an accelerated coordinate system, in which the sinusoidally excited chip remained at rest. Results obtained by the different models were compared to each other. The advantage of the 2nd approach is its superior simplicity, which results in shorter processing time and lower calculation burden. The processing time according to the 2nd approach was found to be 3 times shorter than that of the 1st approach. We thus suggest considering to perform simulations of cantilever vibration modes within suitably chosen accelerated frames of reference.

**Keywords:** Atomic Force Microscope (AFM), cantilever, piezo, MEMS

## 1 Introduction

An atomic force microscope's (AFM) cantilever is a miniature elastic beam with its characteristic vibration modes. Different vibration modes can be excited by applying harmonic loads from a piezoelectric element.

Vibration modes of a micro cantilever are characterized by numerous eigenmodes, each having its own natural frequency. Raman *et al.* [1] have shown that the main eigenmodes consist of bending eigenmodes transverse to the plane of the cantilever and of torsional modes. Experimental measurements aiming at characterizing the dynamics of the AFM cantilevers are limited by by the miniature dimensions of the beam. Some methods of determining the local vibration amplitudes for cantilevers vibrating in the flexural modes have been described. Examples of this include physical measurements using an optical beam detection sensor [2] and a locally resolving setup using a Michelson heterodyne interferometer [3]. Numerical methods have also been applied in analyzing the vibrations of different types of cantilevers [4] [5]. This current work describes the process of modeling the dynamics of such a cantilever beam using finite element methods and analytical ideas in order to reduce processing load and time.

## 2 Experiments, Computing System

In the dynamic AFM application mode, the cantilever is externally oscillated at or close to its resonance frequency. The oscillation amplitude, phase and resonance frequency are modified by tip-sample interaction forces; these changes in oscillation with respect to the external reference oscillation provide information about the sample's characteristics. E.g. the topography of a sample surface can be imaged by scanning a tip attached to the cantilever over the surface. The geometrical objects needed to model these dynamics essentially consist of the microscale cantilever with a sharp tip (probe), a piezo element and an aluminum holder. Fig. 1 shows these three components.

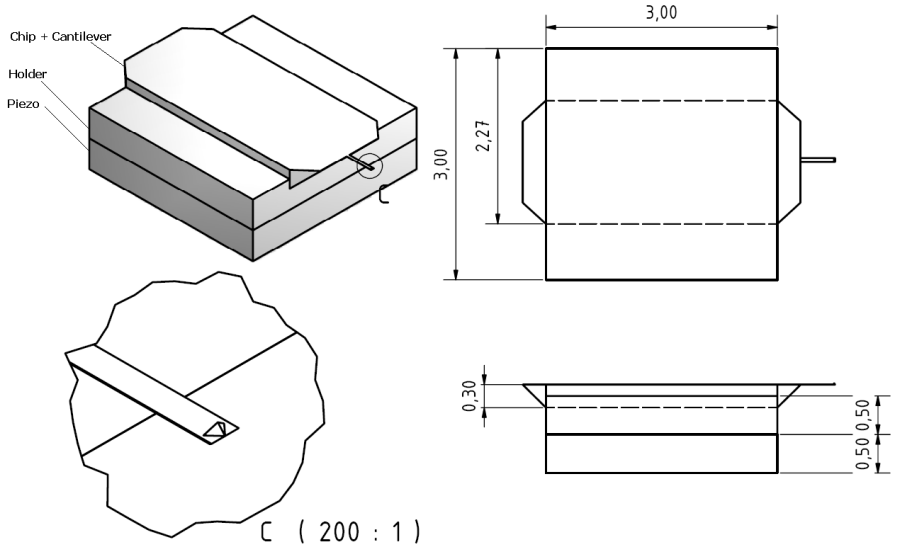


**Fig. 1:** CAD Model of the geometry objects.The dimensions are given in millimeters.

Throughout this paper a cantilever of dimensions length $L = 450\mu m$, width $W = 50\mu m$ and thickness $T = 2\mu m$ was investigated, which was built from crystalline silicon. In the experimental setup corresponding to the models the cantilever was excited by a 0.5 mm thick piezo plate of the ceramic PIC255 produced by PI (Physik Instrumente GmbH & Co. KG, Karlsruhe/Palmbach, Germany). Piezo material data for PIC255 were unavailable from PI, however, and we followed the recommendation of PI to use the data of PIC155 in simulations instead, which was said to show up a very similar behavior. The computing system used for simulations comprised as hardware an AMD Athlon 64 X2 Dual Core 3800+ processor operated at 2 GHz and 3.25 GB RAM. The system was operated by Microsoft Windows XP Professional, Version 2002, SP2 (32-bit version), and the software COMSOL 3.4.0.250 together with MatLab 7.1.0.246 (R14), SP3 was installed.

# 3 Models

## 3.1 Model 1

With the aim of realizing a numerical procedure for solving the continuum mechanics of all the components described in Fig. 1, all their physical and dynamical aspects had to be considered and duly described. This subsection gives an insight of the major aspects that were crucial in development of the first model, which involved two different COMSOL modules, the structural mechanics module and the MEMS module.

Options of both modules were combined in a single multiphysics model such that a *solid, stress-strain* domain from COMSOL's structural mechanics package and a *piezo solid* domain from the MEMS package was built. The geometrical components were designed using Autodesk Inventor and imported into the COMSOL environment using the *CAD import tool*. A set of boundary conditions was introduced in order to correctly couple the different compounds of the model. These consisted of two mechanical and one electrical boundary conditions. One of the former conditions consisted in the fixation of the chip-holder to the piezo element. The other mechanical boundary condition specified the fixation of the lower surface of the piezo element. The piezo's axis of polarization was defined to be along the z-axis. The electrodes were defined such that the electric field across the element had only a z-component. Due to these conditions the piezo was excited mainly to vibrations in z-direction. The uppermost face for the piezo was defined as the ground potential thereby realizing the electrical boundary condition.

The load versus response behavior is crucial in any FEM model. This mainly depends on the material properties of all components within the system. The matrices

containing material property data of the mechanical components were imported from COMSOL's material library. Data matrices of the PIC 155 piezo element used in this model are presented in (1), (2) and (3), where $c_E$ is the elasticity matrix, $e$ the coupling matrix and $\epsilon_S$ the relative permittivity.

$$c_E = \begin{bmatrix} 10.1 & 6.33 & 6.33 & 0 & 0 & 0 \\ 6.33 & 10.1 & 6.33 & 0 & 0 & 0 \\ 6.33 & 6.33 & 1.01 & 0 & 0 & 0 \\ 0 & 0 & 0 & 1.91 & 0 & 0 \\ 0 & 0 & 0 & 0 & 1.91 & 0 \\ 0 & 0 & 0 & 0 & 0 & 2.38 \end{bmatrix} \times 10^{10} Pa \tag{1}$$

$$e = \begin{bmatrix} 0 & 0 & 0 & 0 & 10.3 & 0 \\ 0 & 0 & 0 & 10.3 & 0 & 0 \\ -5.6 & -5.6 & 12.8 & 0 & 0 & 0 \end{bmatrix} \times \frac{C}{m^2} \tag{2}$$

$$\epsilon_S = \begin{bmatrix} 873 & 0 & 0 \\ 0 & 873 & 0 \\ 0 & 0 & 680 \end{bmatrix} \tag{3}$$

## 3.2 Model 2

The design of the second model aims at a simplification of the simulation process. For this purpose a frame of reference is chosen such that the sinusoidally excited contact area of the piezo and the cantilever chip stays at rest within this frame (Fig. 1(b)). The multiphysics model in this case was set using only the *solid, stress-strain* option. The fix position of the contact area points represents the only boundary condition to be considered within this model. Since the simulation no longer takes place in an inertial system but in an accelerated frame of reference, fictitious forces $F_f$ have to be taken into account.

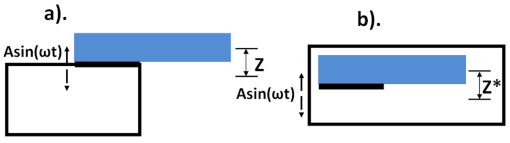


Figure 1: Schematic representation of the inertial system (a) and the accelated frame of reference system (b) as defined for model 1 and 2 respectively. Blue rectangle: Chip plus cantilever.

The vertical coordinates $z$, $z^*$ within the two different frames of reference are related via

$$z = z^* + Asin(\omega t) \tag{4}$$

The vertical dynamics of a mass element $m$ in the inertial system (Fig. 1(a)) is described by Newtons second law

$$F_z = m\ddot{z} \tag{5}$$

where $F_z$ denotes the vertical component of the sum of all forces acting on the mass. In general $F_z$ can be categorized into internal forces (elastically transmitted through the material) and external forces (electric, magnetic, frictional, viscous, gravitational). For the treatment in this paper we neglect all external forces besides those acting on the boundary between the chip and piezo due to excitation. Insertion of equation (4) into equation (5) leads to

$$F_z = m\ddot{z^*} - mA\omega^2 \sin(\omega t),$$

which can be converted to

$$F_z^* := F_z + mA^2 \sin(\omega t) = m\ddot{z^*}. \tag{6}$$

Equation (6) represents Newtons second law in the accelerated frame of reference. Here one has to take into account a fictitious force $F_f = mA\omega^2 \sin(\omega t)$ in addition to the forces $F_z$ present in the inertial system. Instead of forces $F$ one considers loads $L_z := F_z/V$ in continuum mechanics, where V denotes a volume element. Hence Newtons second law reads in terms of loads

$$L^* := L_z + L_f = \rho\ddot{z^*} \tag{7}$$

with the load $L_z := F_z/V$, the fictitious load $L_f := \rho A\omega^2 \sin(\omega t)$ and the material density $\rho := m/V$. It is worthwhile to note that the fictitious load depends on the excitation frequency $\omega$.

During the simulation the fictitious load was calculated and updated after each step in excitation frequency. The excitation amplitude was kept constant at a value $A$, defined as the average value of the vibration amplitudes of the contact points on the interface between the holder and the chip in model 1.

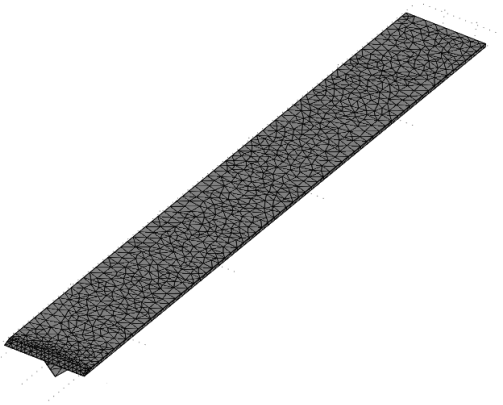

Figure 2: Geometry of the meshed single-silicon cantilever beam with a pyramidal tip.

# 4 Methods

The relation between displacement and strain is essential in the formulation of FEM elements [6]. Strain can be defined as the geometrical expression of displacements caused by the action of stress on a physical body. Nodal displacements ($u$, $v$ and $w$) were the primary unknowns in this work. The stress field in both, model 1 and 2, originated from the vibration of the piezo element. The shear and normal strain present on the chip and the cantilever were therefore known. They were determined through the calculation of internal stresses within the piezo element. From the strain-displacement relations the displacements sought could be determined. These relations can be stated in matrix-operator form according to [6] as

$$\begin{Bmatrix} \epsilon_x \\ \epsilon_y \\ \epsilon_z \\ \gamma_{xy} \\ \gamma_{yz} \\ \gamma_{zx} \end{Bmatrix} = \begin{bmatrix} \frac{\partial}{\partial x} & 0 & 0 \\ 0 & \frac{\partial}{\partial y} & 0 \\ 0 & 0 & \frac{\partial}{\partial z} \\ \frac{\partial}{\partial y} & \frac{\partial}{\partial x} & 0 \\ 0 & \frac{\partial}{\partial z} & \frac{\partial}{\partial y} \\ \frac{\partial}{\partial z} & 0 & \frac{\partial}{\partial x} \end{bmatrix} \begin{Bmatrix} u \\ v \\ w \end{Bmatrix}, \tag{8}$$

where $\epsilon$ and $\gamma$ represent normal and shear strain respectively. Within COMSOL's structural mechanics package there are well defined and highly optimized tools for solving such systems. After a thorough definition of the model and the boundary conditions within the COMSOL environment as discussed in the previous sections a solver routine was run to compute the solution. Nodal displacements along the z-axis of the cantilever beam were of special interest. These displacements were used to determine the cantilever displacement amplitudes and its resonance frequency. To arrive at this information, calculations were made for a number of frequencies using the frequency response option.

Essentially the electro-mechanical FEM equations representing piezoelectric materials are summarized into a couple of equations and are grouped into two categories. These are the stress-charge form and the strain-charge form. The former is defined within COMSOL as

$$\mathbf{T} = c_E S - e\mathbf{E} \tag{9}$$

$$\mathbf{D} = e + \epsilon_S \mathbf{E}, \tag{10}$$

where $T$ is the stress vector, $S$ the strain vector, $E$ the electric field vector, $D$ the electric flux density vector, $c_E$ the elasticity matrix, $e$ the piezoelectric coupling matrix in stress-charge form and $\epsilon_S$ the matrix of relative permittivity. The stress-charge form is used throughout this work. Material characteristics are stored in the matrices $c_E$, $e$ and $\epsilon_S$, which are presented in (1), (2) and (3).

In model 2, since the fictitious force depends on the excitation frequency, the fictitious load $L_f$ had to be calculated iteratively for each calculation step. The frequency response was therefore implemented in MatLab. Values of $L_f$ were calculated at initialization and then passed on to an automatically generated COMSOL script in vector form. In the calculation a loop was implemented using frequency as the loop variable. For each frequency step the respective value of $L_f$ was read, the solution was calculated and the results were saved in a matrix. At the end of the for loop the results were assigned to the *fem.sol* structure for post-processing purposes.

# 5 Results and Discussion

By analytical methods the flexural natural frequencies of a cantilever can be calculated [5]. Using the cantilever geometry described in Section 2 and the silicon material properties density $\rho = 2.33 g/cm^3$ and Young's modulus $E = 169 GPa$ we arrived at a frequency

$$f^{(1)}_{theo} = 13.586 kHz$$

for the first vertical flexural natural mode. This calculated value is located in the resonance frequency specification range $f^{(1)}_{manuf} = (13 \pm 4)kHz$ stated by the manufacturer of the cantilever. In the neighborhood of this value simulations were performed within the frequency response option of COMSOL. Fig. 1 shows the simulated amplitude of a point at the end of the cantilever in dependence on frequency. Clearly a peak at $f^{(1)}_{model1} = (13600 \pm 5)Hz$ is visible. The simulation time for the 40 data points amounted to $t_{model1} = 54min$. Furthermore the displacement amplitudes of points on the cantilever surface at the frequency $f^{(1)}_{model1}$ are shown in Fig. 2. The figure clearly indicates that the cantilever vibrates in the first vertical flexural natural mode.

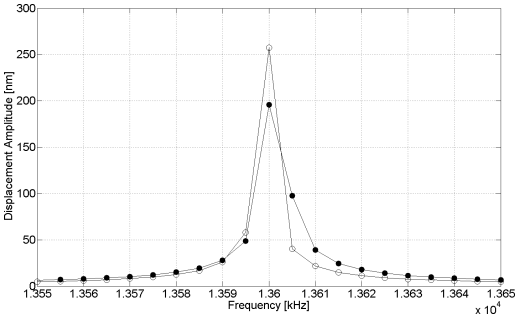


Figure 1: Amplitude of the end of the cantilever vs. excitation frequency. Solid circles: model 1. Open circles: model 2. Solid lines just serve as a guide to the eye.

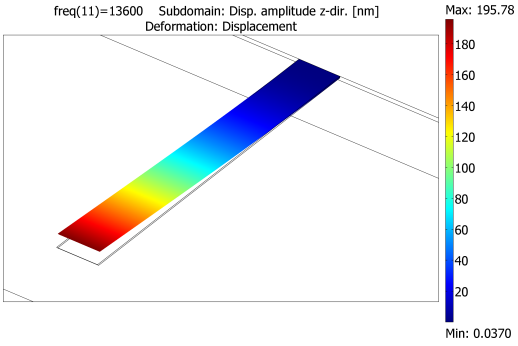


Figure 2: Displacement amplitudes of the cantilever vibrating at 13600Hz. Simulation based on model 1. (Deformation exaggerated due to specification of the deformed shape option.)

The results within model 1 were compared to simulations based on model 2. In order to match the simulations within the 2 models, one has to determine the amplitude $A$ of oscillation in model 1 and feed this value into the simulations according to model 2. We observed that the piezo amplitude delicately depends on the boundary conditions, describing how the piezo is embedded within its environment. A freely oscillating piezo plate of the material PIC155 is ideally expected to vibrate with an amplitude $A_{theo} = d_{33} \cdot 0.5V = 3.07 \times 10^{-10} m/V \cdot 0.5V = 0.1535nm$. However, in a system where the piezo plate is fixed with its surfaces to other components the vibration amplitude is substantially decreased. Furthermore deformations of other parts of the system, e.g. the aluminum holder plate, also have to be taken into account. Fig. 3 shows that as well the piezo plate as the aluminum holder deform in directions parallel to the piezo plate surfaces. In our simulated system the vibration amplitude at 0.5 V excitation voltage and 13.6 kHz excitation frequency amounted to $A_{sim,piezo} = 0.0395nm$ measured at the upper piezo surface and $A_{sim,holder} = 0.0430nm$ measured at the fixation points between the holder plate and the cantilever chip. Further the value $A_{sim,holder}$ was used as basis within model 2.

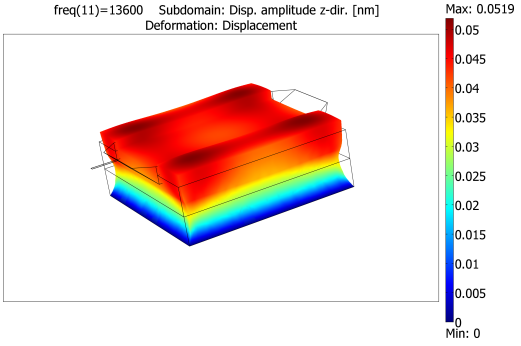


Figure 3: Displacement amplitude in z-direction of piezo plate and aluminum cantilever holder. (Deformation exaggerated due to specification of deformed shape option.) The total system was simulated according to model 1 at 13.6 kHz, cantilever and chip components are suppressed within the figure.

Results of simulations according to model 2 are included in Fig. 1. They match well the results based on model 1 and show up a similar resonance frequency peak at $f^{(1)}_{model2} = (13600 \pm 5)Hz$. Simulation time amounted to $t_{model2} = 16min$. In conclusion the ratio of processing times of simulations following the 2 models is determined as $t_{model1}/t_{model2} = 3.375 \approx 3$.

The amplitude values obtained by both models near the resonance frequency show differences. At the resonance frequency of 13600Hz a relative deviation $(250 - 200)/250 = 20\%$ occurs and at 13605Hz the deviation is even more than a factor 2, but reversed. Based on the definition of the coordinate system in model 2 the amplitudes derived within this model are expected to be by $A = 0.0430nm$ smaller than the ones derived by model 1. Compared to amplitude values of more than 100 nm obtained by simulation near the resonance frequency, however, this correction can be neglected. We rather expect that numerical inaccuracies sum up differently within the two models especially near the resonance. As damping of the cantilever was neglected in both models amplitudes diverging to infinity are expected for frequencies near the resonance. A proper treatment of the system should include damping, however, damping was neglected, as it exceeded the capacity of the computer system in the used configuration.

Resonance frequencies determined by simulations according to the 2 models agree well with the analytically derived frequency $f^{(1)}_{theo}$. The difference $f^{(1)}_{model1} - f^{(1)}_{theo} = 14Hz$ of 0.1% can mainly be attributed to numerical inaccuracies due to the usage of finite elements.

# 6 Conclusions

Due to surging interests in operating an AFM in atmospheric or aqueous environment, complex simulation models are becoming more and more crucial. The complexity however considerably increases the computational burden. Therefore a method of diminishing processing load in simulations by choosing a suitable accelerated coordinate system was developed in the work presented in this article. The first vertical flexural resonance of a cantilever was simulated within different frames of reference. Within both models the estimated resonance frequencies $f^{(1)}_{model1} = f^{(1)}_{model2} = (13600 \pm 5)Hz$ excellently agree with each other. They also agree well with the analytically derived resonance frequency $f^{(1)}_{theo} = 13586Hz$ calculated by the formula for a clamped-free rectangular beam. The amplitudes derived by the two models, however, largely disagree near the resonance frequency. We attribute the differences mainly to the missing implementation of damping within the simulations. Processing time of simulations in an accelerated coordinate system according to model 2 was more than a factor 3 shorter than for simulations in model 1. Combined with other known solutions, which help to ease calculation load, the presented method can aid in decreasing the computing load and processing time in simulations of AFM cantilever vibrations.

# References


[1] A. Raman, J. Melcher, and R. Tung, *Cantilever dynamics in atomic force microscopy,* Nanotoday, Vol. 3, 20 (2008)

[2] W. W. Clegg, D. F. L. Jenkins, and M. J. Cunningham, *The preparation of piezoceramicpolymer thick films and their application as micromechanical actuators,* Sensors and Actuators, Vol. 58, 173 (1997)

[3] U. Rabe, K. Janser, and W. Arnold, *Vibrations of free and surface-coupled atomic force microscope cantilevers: Theory and experiment*, Rev. Sci. Instrum., Vol. 67, 3281 (1996)

[4] C. C. Chou, *et al.*, *Simulation of an atomic force microscopy's Probe considering damping effect,* Proceedings excerpt, COMSOL users conference Taipei (2007)

[5] U. Rabe, S. Hirsekorn, M. Reinsteadtler, T. Sulzbach, Ch. Lehrer and W. Arnold, *Influence of the cantilever holder on the vibrations of AFM cantilevers*, Nanotechnology., Vol. 18, 1 (2007)

[6] R. D. Cook, *Concepts and Applications of Finite Element Analysis,*3rd ed., John Wiley and Sons, New York (1989)

[7] COMSOL 3.4, *Multiphysics Users Guide,* COMSOL Version 3.4 (2007)

[8] G. Scheerschmidt, K. J. Kirk, and G. McRobbie *Finite Element Analysis of Resonant Frequencies in Sur-*

*face Acoustic Wave Devices,* COMSOL Users Conference, Birmingham (2006)

## Acknowledgements

This work was supported by the Deutsche Forschungsgemeinschaft in project NanoLatVib (FA 347/24-1).